



UNIVERSIDADE FEDERAL DE MINAS GERAIS
Programa de Pós-Graduação em Engenharia Mecânica

**METHODOLOGY FOR ANALYSIS OF BOUNDARY CONDITIONS IN ORDER TO
INCREASE ACCURACY ASSOCIATED TO INTERNAL COMBUSTION ENGINE
CFD 3D MODELS**

LEONARDO GUIMARÃES FONSECA

Belo Horizonte
2019

Leonardo Guimarães Fonseca

**METHODOLOGY FOR ANALYSIS OF BOUNDARY CONDITIONS IN ORDER TO
INCREASE ACCURACY ASSOCIATED TO INTERNAL COMBUSTION ENGINE
CFD 3D MODELS**

Tese apresentada ao Programa de Pós-Graduação em Engenharia Mecânica da Universidade Federal de Minas Gerais , como requisito parcial à obtenção do título de Doutor em Engenharia Mecânica.

Área de Concentração: Energia e Sustentabilidade

Orientador: Prof. Dr. Ramon Molina Valle

Belo Horizonte
2019

Leonardo Guimarães Fonseca

METHODOLOGY FOR ANALYSIS OF BOUNDARY CONDITIONS IN ORDER
TO INCREASE ACCURACY ASSOCIATED TO INTERNAL COMBUSTION ENGINE
CFD 3D MODELS/ Leonardo Guimarães Fonseca. – Belo Horizonte, 2019–
156 p. : il. (algumas color.) ; 30 cm.

Supervisor: Prof. Dr. Ramon Molina Valle

Tese – Universidade Federal de Minas Gerais , 2019.

1. cfd 3d. 2. rans. 3. internal combustion engines. 4. intake pressure. 5. wall temperature. I. Universidade Federal de Minas Gerais. II. Escola de Engenharia.
III. METHODOLOGY FOR ANALYSIS OF BOUNDARY CONDITIONS IN ORDER
TO INCREASE ACCURACY ASSOCIATED TO INTERNAL COMBUSTION ENGINE
CFD 3D MODELS



UNIVERSIDADE FEDERAL DE MINAS GERAIS
PROGRAMA DE PÓS-GRADUAÇÃO EM
ENGENHARIA MECÂNICA
Av. Antônio Carlos, 6627 - Campus Universitário
31270-901 – Belo Horizonte – MG
Tel.: +55 31 3409.5145
E-mail: cpgmec@demec.ufmg.br

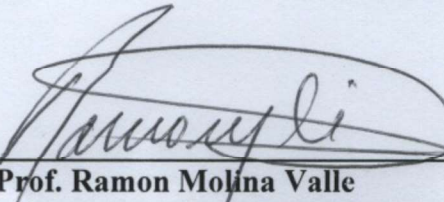
**"METHODOLOGY FOR ANALYSIS OF BOUNDARY CONDITIONS IN
ORDER TO INCREASE ACCURACY ASSOCIATED TO INTERNAL
COMBUSTION ENGINE CFD 3D MODELS"**

LEONARDO GUIMARÃES FONSECA

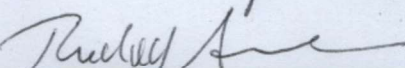
Tese submetida à Banca Examinadora designada pelo Colegiado do Programa de Pós-Graduação em Engenharia Mecânica da Universidade Federal de Minas Gerais, como parte dos requisitos necessários à obtenção do título de "**Doutor em Engenharia Mecânica**", na área de concentração de "**Energia e Sustentabilidade**".

Tese aprovada no dia 03 de outubro de 2019.

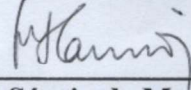
Por:


Prof. Ramon Molina Valle

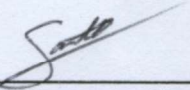
Orientador - Departamento de Engenharia Mecânica/ UFMG


Prof. Rudolf Huebner

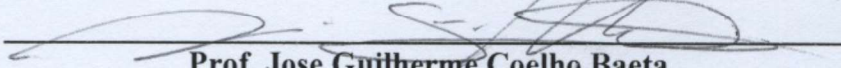
Departamento de Engenharia Mecânica/ UFMG


Prof. Sérgio de Moraes Hanriot

Departamento de Engenharia Mecânica/ PUC-MINAS


Prof. André Augusto Campagnole dos Santos

Centro de Desenvolvimento da Tecnologia Nuclear/ CDTN


Prof. Jose Guilherme Coelho Baeta

Departamento de Engenharia Mecânica/ UFMG

Aos meus pais, Lincoln e Vânia;

Às minhas avós, Alvicina(in memoriam) and Terezinha(in memoriam).

ACKNOWLEDGEMENTS

The author acknowledge the following persons and institutions, for their fundamental role in this work:

- CTM-UFGM, for the infrastructure which was made available for the implementation of this thesis;
- CAPES (Coordination for the Improvement of Higher Education Personnel) for the scholarship from the program "CAPES - DEMANDA SOCIAL", PhD level;
- FCA Latin America, for the research project in partnership with UFGM, the very begining of this project;
- DTEM/UFSJ (Telecommunications and Mechatronic Engineering Department - Federal University of São João del-Rei), for the support conceived to this thesis since may 2018;
- CMT - Motores Térmicos, for the partnership and for the hospitality;
- Prof. Ramon Molina, for his support since the master degree;
- Prof. Rudolf Huebner, for his support since the under graduation simulation projects;
- Prof. Sérgio de Moraes Hanriot, Dr. André Augusto Campagnole dos Santos, Prof. José Guilherme Coelho Baeta, for their contribution to this thesis;
- Prof. Ricardo Novella and Prof. Pablo Olmeda, for the partnership and for the good work performed together;
- Prof. Guilherme Gomes, for the support concerning my dedication to this project.

The author is very grateful.

AGRADECIMENTOS

Primeiramente, agradeço a Deus, princípio, meio e fim de todas as coisas, a luz mais brilhante na caverna mais sombria. A cada conquista, seja sempre o primeiro agradecimento do coração, dar glórias a Deus no mais alto dos céus!!!

À minha esposa Jéssica, companheira de todos os momentos, dos mais fáceis aos mais sombrios. O meu está concluído, agora está com você princesa, é a sua vez!

Aos meus pais, Lincoln e Vânia, as joias mais raras que Deus presenteou a mim e a meus irmãos Flávia, Rodrigo e Lucas. Minha família, meu refúgio, minha rocha e proteção, abrigo durante as tempestades, as muitas que aconteceram nos últimos 4 anos. Aos meus tios e primos, Virgínia, Gilmar, Dudu e Elisa, Anderson, Patrícia, Heitor e Henrique, com quem estou imensamente em falta, mas espero me redimir!

Às minhas avós, Alvicina (*in memorian*) e Terezinha (*in memorian*), que deixaram mais que ensinamentos e exemplos, deixaram um legado de caráter, determinação, obstinação e perseverança, que caminharam tanto conosco antes do início deste processo, mas que durante este processo concluíram suas jornadas.

Aos colegas do CTM, Oscar, Carlos, Vinícius Gaúcho, Vinícius Rimsa, Lucimar, Natalia, Arthur, José Arthur, Bryan, Juan, que compartilharam momentos difíceis e confraternizações ao longo dos últimos anos.

Aos colegas do LCFD, Raphael, Clarissa e Filipe, os herdeiros deste legado em simulação CFD 3D de motores de combustão interna.

Ao secretário do CTM, Alexandre, sempre um bom amigo, nas horas fáceis, difíceis, sempre eficiente e fiel ao CTM.

Ao Prof. Ramon Molina e Ao Prof. Rudolf Huebner, mais que exemplos, grandes amigos, os únicos que ousaram acreditar neste projeto, quando todos os demais acreditaram que eu deveria desistir.

Aos colegas do DETEM/UFSJ, Guilherme, Edgar, Rina, Tarsis, Cláudio, Leandro, Diego, Alfredo, muito trabalho, muitos desafios e muitas alegrias nos aguardam. Vamos juntos!

De modo geral, a todas as pessoas que contribuíram comigo durante este processo, e que não tiveram seus nomes citados acima...

MUITO OBRIGADO!!!

"...rise and rise again, until lambs become lions..." (Autor desconhecido. Robin Hood, 2010.)

ABSTRACT

The use of internal combustion engine simulation models for aiding the development of more efficient and less pollutant engines is by so far known. Engine CFD 3D models are a new tool for this development, although its methodology still needs some improvement in order to systematically produce accurate results. In this thesis, a method for analysis and treatment of boundary conditions for engine CFD 3D models using RANS approach is presented, which should be capable of producing accurate results for different engine operating conditions using the same values for all of the constants of the sub models for turbulence, spray and combustion, so the engine CFD 3D model would be used in a systematic and repetitive way. For intake pressure boundary conditions, a correction for pulsating flow effects is applied, and for wall temperature, the engine CFD 3D results for heat transfer coefficient are used decoupled iteratively with a zero dimensional heat transfer model. The method is applied to a naturally aspirated single cylinder research engine available at CTM-UFMG, fueled with commercial ethanol, for which geometry information and experimental data are available. For the engine CFD 3D model with experimental data intake pressure boundary conditions, the results obtained for injected mass of fuel, lambda and trapped mass of air are compared to experimental data, and excess of air is observed for six different engine operating conditions. The results obtained by the engine CFD 3D model, using corrected intake pressure boundary conditions, are presented for injected mass of fuel, lambda and trapped mass of air for six different engine operating conditions, using two different sets of wall temperature boundary conditions calculated by the zero dimensional heat transfer model. For all of those results, the difference to experimental correlated data is systematically reduced in comparison with the direct use of experimental data for intake pressure boundary conditions. In cylinder pressure trace is compared between experimental data and three different sets of boundary conditions for two selected engine operating conditions, once the trends observed for the selected conditions are representative. The results obtained by the proposed method present better agreement to experimental correlated data than the direct use of experimental data for intake pressure boundary condition, specially during compression and expansion strokes. It is concluded that for this specific naturally aspirated engine, pressure correction of intake experimental boundary conditions is mandatory for performing engine CFD 3D modelling using RANS approach. Once the method has been applied in only one engine, it is only possible to infer, and not to state, that pressure correction of intake experimental boundary conditions is mandatory for this application.

Keywords: CFD 3D, RANS, Internal Combustion Engines, Intake Pressure, Wall Temperature

RESUMO

O uso de modelos para simulação de motores de combustão interna, com objetivo de desenvolver motores mais eficientes e menos poluentes, é prática comum tanto na indústria quanto nos centros de pesquisa. Modelos CFD 3D para motores de combustão interna são uma nova ferramenta para esta aplicação, contudo sua metodologia ainda precisa de algum desenvolvimento para produzir sistematicamente resultados confiáveis. Nesta tese, é apresentada uma metodologia para análise das condições de contorno implementadas em modelos CFD 3D de motores de combustão interna que utilizam o tratamento RANS para turbulência, sendo que esta metodologia deve ser capaz de produzir resultados confiáveis para diferentes condições de operação do motor utilizando sempre os mesmos valores para todas as constantes dos sub modelos relacionados a turbulência, "spray" e combustão. Para condições de contorno de pressão na admissão, uma correção é aplicada aos dados experimentais devido ao efeito do escoamento pulsante na admissão, enquanto para as temperaturas de parede, os resultados do modelo CFD 3D para coeficiente de transferência de calor são usados de forma iterativa desacoplada com um modelo de transferência de calor zero dimensional. A metodologia é aplicada a um motor monocilindro de pesquisa aspirado disponível no CTM-UFGM, utilizando etanol comercial, em relação ao qual informações sobre geometria e dados experimentais foram disponibilizados para esta pesquisa. Para o modelo CFD 3D utilizando dados experimentais como condição de contorno de pressão na admissão, os resultados obtidos para massa de combustível injetada, lambda e massa de ar aprisionada são comparados com dados experimentais, e é constatado excesso de ar para seis diferentes condições de operação do motor. Os resultados obtidos pelo modelo CFD 3D, utilizando pressão corrigida como condição de contorno na admissão, são apresentados para massa de combustível injetada, lambda e massa de ar aprisionada para todos os casos, usando dois tipos de condição de contorno de temperatura de parede calculados pelo modelo zero dimensional de transferência de calor. Para todos os resultados, a diferença em relação aos dados experimentais correlatos é sempre menor que a obtida pelo uso direto dos dados experimentais de pressão na admissão como condição de contorno. Os resultados do modelo CFD 3D utilizando pressão corrigida como condição de contorno na admissão também apresentam melhor correlação com dados experimentais correlatos em comparação com os obtidos pelo mesmo modelo usando diretamente dados experimentais para a mesma condição de contorno, em termos do comportamento da pressão dentro do cilindro ao longo do ciclo e da temperatura dentro do cilindro ao longo do ciclo. Conclui-se que para o motor monocilindro aspirado em análise, a correção da condição de contorno de pressão na admissão é obrigatória para a modelagem CFD 3D de motores de combustão interna utilizando tratamento RANS para turbulência.

Palavras chave: CFD 3D, RANS, Motores de Combustão Interna, Pressão da Admissão, Temperatura de Parede

LIST OF FIGURES

Figure 2.1 – Grid generation process at ES-ICE module.	36
Figure 2.2 – Schematic of ECFM-3Z model.	38
Figure 2.3 – Hollow-cone spray break-up diagram.	40
Figure 3.1 – Engine test bench.	63
Figure 3.2 – Engine parts assembled in a CAD drawing.	65
Figure 3.3 – Geometry of the simulation domain, which consists in the volume of fluid regions inside intake manifold, intake port, in cylinder, exhaust port and exhaust manifold.	66
Figure 3.4 – Complete simulation grid at bottom dead center, for the grid 1 with a characteristic length of 1 mm.	67
Figure 3.5 – Example of experimental data for intake and exhaust pressure traces.	73
Figure 3.6 – Thermal resistance diagram for global heat transfer model.	76
Figure 3.7 – Simulation methodology block diagram, comprising the decoupled iterative method between engine CFD 3D and global HT models.	88
Figure 4.1 – Results for in cylinder pressure trace obtained by engine CFD 3D model using different sets of boundary conditions, in comparison to experimental correlated data. Engine operating condition is 2000 rpm 3 bar, domain between -360 CAD and 360 CAD, range from 0 bar to 30 bar.	110
Figure 4.2 – Results for in cylinder pressure trace obtained by engine CFD 3D model using different sets of boundary conditions, in comparison to experimental correlated data. Engine operating condition is 2000 rpm 3 bar, domain between -360 CAD and 0 CAD, range from 0.2 bar to 1.2 bar.	112
Figure 4.3 – Results for in cylinder pressure trace obtained by engine CFD 3D model using different sets of boundary conditions, in comparison to experimental correlated data. Engine operating condition is 2000 rpm 3 bar, domain between 0 CAD and 360 CAD, range from 0.5 bar to 2.5 bar.	113
Figure 4.4 – Results for in cylinder pressure trace obtained by engine CFD 3D model using different sets of boundary conditions, in comparison to experimental correlated data. Engine operating condition is 2000 rpm 3 bar, domain between -30 CAD and 90 CAD, range from 0 bar to 30 bar.	114
Figure 4.5 – Pressure volume diagram for in cylinder pressure trace obtained by engine CFD 3D model using different sets of boundary conditions, in comparison to experimental correlated data. Engine operating condition is 2000 rpm 3 bar.	115
Figure 4.6 – Pressure logarithm versus volume logarithm diagram for in cylinder pressure trace obtained by engine CFD 3D model using different sets of boundary conditions, in comparison to experimental correlated data. Engine operating condition is 2000 rpm 3 bar.	116

Figure 4.7 – Results for in cylinder temperature trace obtained by engine CFD 3D model using different sets of boundary conditions, in comparison to experimental correlated data. Engine operating condition is 2000 rpm 3 bar, domain between -30 CAD and 90 CAD, range from 300 K to 2100 K.	117
Figure 4.8 – Results for in cylinder pressure trace obtained by engine CFD 3D model using different sets of boundary conditions, in comparison to experimental correlated data. Engine operating condition is 2000 rpm 8 bar, domain between -360 CAD and 360 CAD, range from 0 bar to 60 bar.	119
Figure 4.9 – Results for in cylinder pressure trace obtained by engine CFD 3D model using different sets of boundary conditions, in comparison to experimental correlated data. Engine operating condition is 2000 rpm 8 bar, domain between -360 CAD and 0 CAD, range from 0.6 bar to 1.6 bar.	120
Figure 4.10–Results for in cylinder pressure trace obtained by engine CFD 3D model using different sets of boundary conditions, in comparison to experimental correlated data. Engine operating condition is 2000 rpm 8 bar, domain between 0 CAD and 360 CAD, range from 0.5 bar to 5.5 bar.	121
Figure 4.11–Results for in cylinder pressure trace obtained by engine CFD 3D model using different sets of boundary conditions, in comparison to experimental correlated data. Engine operating condition is 2000 rpm 8 bar, domain between -30 CAD and 90 CAD, range from 0 bar to 60 bar.	122
Figure 4.12–Pressure volume diagram for in cylinder pressure trace obtained by engine CFD 3D model using different sets of boundary conditions, in comparison to experimental correlated data. Engine operating condition is 2000 rpm 8 bar.	123
Figure 4.13–Pressure logarithm versus volume logarithm diagram for in cylinder pressure trace obtained by engine CFD 3D model using different sets of boundary conditions, in comparison to experimental correlated data. Engine operating condition is 2000 rpm 8 bar.	124
Figure 4.14–Results for in cylinder temperature trace obtained by engine CFD 3D model using different sets of boundary conditions, in comparison to experimental correlated data. Engine operating condition is 2000 rpm 3 bar, domain between -30 CAD and 90 CAD, range from 500 K to 2500 K.	125
Figure A.1–Geometry of the simulation domain highlighted inside engine parts. Geometry volumes are highlighted for in cylinder (red) and intake and exhaust ducts (blue).	141
Figure A.2–Internal volume geometry details: complete geometry.	142
Figure A.3–Internal volume geometry details: engine head internal volume.	143
Figure B.1 – Template 2D generated for the in cylinder geometry of the evaluated engine. Template corresponding to grid 1, for a characteristic length of 1 mm.	144

Figure B.2 – Instant 3D grid at top dead center, for the grid 1 with a characteristic length of 1 mm.	146
Figure B.3 – Instant 3D grid at bottom dead center, for the grid 1 with a characteristic length of 1 mm.	147

LIST OF TABLES

Table 3.1 – Single cylinder research engine parameters.	62
Table 3.2 – Relevant experimental sensors for simulation procedure. Uncertainties are given in terms of full scale values (FS) or measurement values(M).	63
Table 3.3 – Engine operating conditions.	63
Table 3.4 – Comparison between experiment and model volume and volumetric compression ratio.	65
Table 3.5 – Reference characteristic length for different grids used in this work.	68
Table 3.6 – Grid dependence study results.	69
Table 3.7 – Time step evaluation	70
Table 3.8 – Surface temperatures calculated by the proposed global heat transfer model. .	76
Table 3.9 – Boundary conditions for the global heat transfer model.	77
Table 4.1 – Results for injected mass of fuel calculated by engine CFD 3D model at several cases, using measured intake pressure as intake boundary condition, in comparison with experimental data.	93
Table 4.2 – Results for lambda calculated by engine CFD 3D model at several cases, using measured intake pressure as intake boundary condition, in comparison with experimental data.	93
Table 4.3 – Results for trapped mass of air calculated by engine CFD 3D model at several cases, using measured intake pressure as intake boundary condition, in comparison with experimental data.	94
Table 4.4 – Engine CFD 3D model excess of air, using measured intake pressure as boundary condition, presented in the form of an engine map.	95
Table 4.5 – Results for the pressure correction procedure, for the given engine speed and load combinations.	98
Table 4.6 – Results for pressure correction procedure, presented in the form of an engine map.	98
Table 4.7 – Results for wall surface temperature at all surfaces of the global heat transfer model, for first (1st) and second (2nd) iteration.	99
Table 4.8 – Results for wall surface temperature at all surfaces of the global heat transfer model, for second (2nd) and third (3rd) iteration.	101
Table 4.9 – Surface temperature calculated by the global heat transfer model at second iteration, for all regions considered at all of the engine operating conditions evaluated.	102
Table 4.10–Results for injected mass of fuel calculated by engine CFD 3D model at several cases, using fitted intake pressure as intake boundary condition and first iteration heat transfer model results as wall temperature boundary condition, in comparison with experimental data.	103

Table 4.11—Results for trapped mass of air calculated by engine CFD 3D model at several cases, using fitted intake pressure as intake boundary condition and first iteration heat transfer model results as wall temperature boundary condition, in comparison with experimental data.	103
Table 4.12—Results for lambda calculated by engine CFD 3D model at several cases, using fitted intake pressure as intake boundary condition and first iteration heat transfer model results as wall temperature boundary condition, in comparison with experimental data.	104
Table 4.13—Results for indicated mean effective pressure (IMEP) calculated by engine CFD 3D model at several cases, using fitted intake pressure as intake boundary condition and first iteration heat transfer model results as wall temperature boundary condition, in comparison with experimental data.	105
Table 4.14—Results for peak pressure calculated by engine CFD 3D model at several cases, using fitted intake pressure as intake boundary condition and first iteration heat transfer model results as wall temperature boundary condition, in comparison with experimental data.	105
Table 4.15—Results for injected mass of fuel calculated by engine CFD 3D model at selected cases, using fitted intake pressure as intake boundary condition and second iteration heat transfer model results as wall temperature boundary condition, in comparison with experimental data.	107
Table 4.16—Results for trapped mass of air calculated by engine CFD 3D model at selected cases, using fitted intake pressure as intake boundary condition and second iteration heat transfer model results as wall temperature boundary condition, in comparison with experimental data.	107
Table 4.17—Results for lambda calculated by engine CFD 3D model at selected cases, using fitted intake pressure as intake boundary condition and second iteration heat transfer model results as wall temperature boundary condition, in comparison with experimental data.	108
Table 4.18—Results for indicated mean effective pressure (IMEP) calculated by engine CFD 3D model at selected cases, using fitted intake pressure as intake boundary condition and second iteration heat transfer model results as wall temperature boundary condition, in comparison with experimental data.	109
Table 4.19—Results for peak pressure (P_{MAX}) calculated by engine CFD 3D model at selected cases, using fitted intake pressure as intake boundary condition and second iteration heat transfer model results as wall temperature boundary condition, in comparison with experimental data.	109
Table 4.20—Results calculated by engine CFD 3D model using different sets of boundary conditions, in comparison to experimental correlated data, for 2000 rpm 3 bar.	118

Table 4.21—Results calculated by engine CFD 3D model using different sets of boundary conditions, in comparison to experimental correlated data, for 2000 rpm 8 bar.	126
Table B.1—Reference characteristic length for different grids used in this work.	144
Table B.2—Reference characteristic length for different regions into the 2D template for the grid 1, with reference characteristic length of 1 mm.	145
Table B.3—Actual characteristic length and grid refinement factor of the 2D template for all of the grids evaluated.	145
Table B.4—Actual characteristic length and grid refinement factor of the 3D grids at TDC and BDC for all of the grids evaluated.	147
Table B.5—Characteristic length h [mm] of the TDC, for different grids, evaluated for total grid and for in cylinder, intake and exhaust regions.	148
Table B.6—Number of cells at TDC, for the total domain, and for in cylinder, intake and exhaust regions.	149
Table B.7—Characteristic length h [mm] of the BDC, for different grids, evaluated for total grid and for in cylinder, intake and exhaust regions.	149
Table B.8—Number of cells at BDC, for the total domain, and for in cylinder, intake and exhaust regions.	150
Table B.9—Computational cost for different grids.	153
Table B.10—Time step evaluation	155

NOMENCLATURE

Abbreviations

CO_2	Carbon Dioxide
NO_X	Generic Nitrogen Oxide
0D	Zero Dimensional
1D	One Dimensional
2D	Two Dimensional
3D	Three Dimensional
AKTIM	Ark and Kernel Tracking Ignition Model
ANSYS	Trade name of ANSYS INC.
ASME	The American Society of Mechanical Engineers.
BDC	Bottom Dead Center
CAD	Crank Angle Degrees
CCV	Cycle to Cycle Variations
CFD	Computational Fluid Dynamics
CFX	Trade name of a commercial software, which actually belongs to ANSYS INC.
CHT	Conjugate Heat Transfer
COV	Co Variance
CTM	<i>Centro de Tecnologia da Mobilidade</i> , (Mobility Technology Center, from Portuguese)
dim	Dimensionless
DISI	Direct Injection Spark Ignition
DNS	Direct Numerical Simulation
ECFM-3Z	Extended Coherent Flame Model - Three Zones
EGR	Exhaust Gas Recirculation

HPC	High Performance Computing
HT	Heat Transfer
ICE	Internal Combustion Engines
IMEP	Indicated Mean Effective Pressure
KIVA	Trade name of an open source software
KIVA-3V	Trade name of an open source software
LES	Large Eddy Simulation
PDF	Probability Density Function
PISO	Pressure Implicit with Splitting of Algorithm
PIV	Particle Image Velocimetry
RANS	Reynolds Averaged Navier Stokes
RNG	Re Normalization Group
SGS	Sub Grid Scale
STAR-CD	Trade name of a commercial software, which actually belongs to SIEMENS GmBH.
TDC	Top Dead Center
THC	Total Hydrocarbon
UFMG	<i>Universidade Federal de Minas Gerais</i> (Federal University of Minas Gerais, from Portuguese)

Greek symbols

α	ECFM-3Z model constant [-]
β	ECFM-3Z model constant [-]
$\delta(Z)$	Probability density function for unmixed air zone [-]
$\delta(Z - 1)$	Probability density function for unmixed fuel zone [-]
$\delta(Z - \bar{Z}^M)$	Probability density function for mixture zone [-]
ε	Dissipation of turbulent kinetic energy [m^2/s^3]

ε_{cyl}	Weighting factor for heat transfer between valve stem surface and port gas flow, for which the reference is the heat transfer modeled as flow past a cylinder
$\bar{\rho}$	Flow field average density [kg/m^3]
ϕ	Generic trasport variable [-]
ϕ_{i+1}	Value of the generic variable ϕ at grid $i + 1$ [-]
ϕ_i	Value of the generic variable ϕ at grid i [-]
Σ	Flame surface density [m^2/m^3]

Latin symbols

\bar{I}	Flow field average total internal energy [kJ]
\bar{P}	Flow field average pressure [Pa]
\bar{T}	Flow field average temperature [K]
\bar{U}	Flow field average velocity component [m/s]
\bar{V}	Flow field average velocity component [m/s]
\bar{W}	Flow field average velocity component [m/s]
\bar{Z}^M	Average Mixture Fraction [-]
$\vec{\bar{U}}$	Flow field average velocity vector [m/s]
A	Air plus Exhaust Gas Recirculation Zone [-]
A_{cc}	Area of the combustion chamber for the global heat transfer model [m^2]
A_{exh}	Area of the exhaust port for the global heat transfer model [m^2]
A_{int}	Area of the intake port for the global heat transfer model [m^2]
$A_{lin,ext}$	Area of cylinder outside surface exposed to coolant flow [m^2]
c	Reaction progress variable [-]
C'_{gal}	Constant in the equation for thermal conductance between piston surface and oil [-]
C_2	Constant in the Woschni equation [-]
C_u	Constant in the Woschni equation [-]

C_{w1}	Constant in the Woschni equation [-]
C_{w2}	Constant in the Woschni equation [-]
D	Generic experimental measurement [-]
D_{curv}	Port curvature diameter [m]
D_{cyl}	Cylinder diameter (bore) in the Woschni equation [m]
D_{gal}	Piston inner diameter in the region of the lubricating oil gallery [m]
d_{gal}	Diameter or hydraulic diameter of the piston lubricating oil gallery [m]
D_{pis}	Piston diameter [m]
D_{port}	Port diameter or hydraulic diameter [m]
E	Generic comparison error [-]
e_{cc}	Thickness of the combustion chamber for the global heat transfer model
e_{exh}	Thickness of the exhaust port for the global heat transfer model
e_{int}	Thickness of the intake port for the global heat transfer model
e_{lin}	Thickness of the cylinder wall for the global heat transfer model
F	Unburned Fuel Zone [-]
h	Grid characteristic length [mm]
h_{coarse}	Characteristic length of a coarse grid [mm]
$h_{cylinder}$	Heat transfer coefficient between valve stem surface and port gas flow, modeled as flow past a cylinder [W/m^2K]
h_{fine}	Characteristic length of a fine grid [mm]
$h_{flatplate}$	Heat transfer coefficient between valve stem surface and port gas flow, modeled as flow past a flat plate [W/m^2K]
$h_{gal-cool}$	Heat transfer coefficient between head cooling gallery surface and coolant flow [W/m^2K]
h_{gas}	Heat transfer coefficient for in cylinder gas [W/m^2K]
$h_{lin-cool}$	Heat transfer coefficient between cylinder outside surface and coolant flow [W/m^2K]

$h_{lin-oil}$	Heat transfer coefficient between cylinder liner surface and oil [W/m^2K]
h_{pc}	Piston ring height [m]
$h_{pis-lin}$	Heat transfer coefficient between piston surface and cylinder liner surface [W/m^2K]
$h_{portcurv}$	Heat transfer coefficient between port surface and port gas flow, for curved tube approximation [W/m^2K]
$h_{stemgas}$	Heat transfer coefficient between valve stem surface and port gas flow [W/m^2K]
$h_{straighttube}(x = \infty)$	Heat transfer coefficient between port surface and port gas flow, for straight tube approximation in fully developed flow [W/m^2K]
k	Turbulent kinetic energy [m^2/s^2]
K_{cc-gal}	Thermal conductance between combustion chamber surface and head cooling gallery surface [W/K]
k_{cc}	Thermal conductivity of the cylinder wall, for the global heat transfer model [$W/m.K$]
k_{cc}	Thermal conductivity of the engine head in the region of the combustion chamber, for the global heat transfer model [$W/m.K$]
$K_{exh-gal}$	Thermal conductance between exhaust port surface and head cooling gallery surface [W/K]
k_{exh}	Thermal conductivity of the engine head in the region of the exhaust port, for the global heat transfer model [$W/m.K$]
$K_{gal-cool}$	Thermal conductance between head cooling gallery surface and coolant flow [W/K]
$K_{gas-head}$	Thermal conductance between in cylinder gases and combustion chamber surface [W/K]
$K_{gas-lin}$	Thermal conductance between in cylinder gases and cylinder liner surface [W/K]
$K_{gas-pis}$	Thermal conductance between in cylinder gases and piston surface [W/K]
$K_{gas-valv}$	Thermal conductance between in cylinder gases and valve surface [W/K]
$K_{int-gal}$	Thermal conductance between intake port surface and head cooling gallery surface [W/K]

k_{int}	Thermal conductivity of the engine head in the region of the intake port, for the global heat transfer model [W/m.K]
$K_{lin-cool}$	Thermal conductance between cylinder liner surface and coolant flow [W/K]
$K_{lin-oil}$	Thermal conductance between cylinder liner surface and oil [W/K]
$K_{pis-lin}$	Thermal conductance between piston surface and cylinder liner surface [W/K]
$K_{pis-oil}$	Thermal conductance between piston surface and oil [W/K]
k_{pis}	Thermal conductivity of the piston, for the global heat transfer model [W/m.K]
M	Mixture Zone [-]
m	Constant in the equation for thermal conductance between piston surface and oil [-]
N	Total number of finite volumes in a grid [-]
$Nu_{cylinder}$	Nusselt number for heat transfer between valve stem and port gas flow, modeled as flow past a cylinder [dim]
$Nu_D(x)$	Nusselt number for heat transfer between port surface and port gas flow, for turbulent entrance length flow [dim]
$Nu_D(x = \infty)$	Nusselt number for heat transfer between port surface and port gas flow, for turbulent fully developed flow [dim]
$Nu_{flatplate}$	Nusselt number for heat transfer between valve stem and port gas flow, modeled as flow past a flat plate [dim]
p_{ivc}	Pressure of the in cylinder gases at intake valve closing [bar]
r	Grid refinement ratio [dim]
Re	Reynolds number [dim]
S	Generic simulation result [-]
S_{cyl}	Cylinder stroke [m]
S_p	Average piston speed for the global heat transfer model [-]
$T_{gas-head}$	Cycle average in cylinder gas temperature, as it is seen by combustion chamber surface [K]

$T_{gas-lin}$	Cycle average in cylinder gas temperature, as it is seen by cylinder liner surface [K]
$T_{gas-pis}$	Cycle average in cylinder gas temperature, as it is seen by piston surface [K]
$T_{gas-valv}$	Cycle average in cylinder gas temperature, as it is seen by valve surface [K]
T_{ivc}	Temperature of the in cylinder gases at intake valve closing [K]
$U_{95\%}$	Uncertainty of a given result, for a 95% confidence interval [-]
V_D	Displaced volume in the Woschni equation [-]
V_{ivc}	Volume of the in cylinder gases at intake valve closing [m^3]
V_i	Volume of the i_{th} cell [mm^3]
x	Port length for heat transfer between port surface and port gas flow [m]
Z	Mixture fraction variable [-]
P_1aIT	Results for in cylinder pressure trace obtained by engine CFD 3D model using fitted intake pressure boundary conditions along with first iteration wall temperatures calculated by global heat transfer model [bar]
P_2aIT	Results for in cylinder pressure trace obtained by engine CFD 3D model using fitted intake pressure boundary conditions along with second iteration wall temperatures calculated by global heat transfer model [bar]
P_envelope	Experimental data for in cylinder pressure, associated to the dispersion of the 200 cycles for in cylinder pressure experimental data [bar]
P_EXP	Experimental data for in cylinder pressure trace [bar]
P_max	Maximum pressure of in cylinder pressure trace (peak pressure) [bar]
P_piexp	Results for in cylinder pressure trace obtained by engine CFD 3D model using experimental data intake pressure boundary conditions along with first iteration wall temperatures calculated by global heat transfer model [bar]

CONTENTS

List of Figures	10
List of Tables	13
Nomenclature	16
Contents	23
1 INTRODUCTION	25
1.1 Engine CFD 3D models	26
1.2 Pulsating effects on intake flow	28
1.3 Wall temperature boundary conditions	29
1.4 Objectives	30
2 LITERATURE REVIEW	32
2.1 Basic Concepts	32
2.2 Engine CFD 3D MODEL	36
2.3 ICE intake manifold pulsating flow	41
2.4 Engine heat transfer modelling	42
2.5 State of the art	44
3 METHODOLOGY	60
3.1 Computational infrastructure	60
3.2 Engine and test bench	62
3.3 Geometry and simulation domain	64
3.4 Grid study	66
3.5 Mathematical physics model	70
3.6 Boundary conditions	73
3.7 Global HT model	75
3.8 Simulation methodology	84
3.9 Presentation of results	87
3.10 Methodology final remarks	90
4 RESULTS AND DISCUSSION	92
4.1 Results for engine CFD 3D model using experimental intake pressure, compared to experimental results	92
4.2 Proposed hypothesis about systematic excess of air	95
4.3 Results for pressure correction	97
4.4 Results for global heat transfer model	99

4.5	Results for engine CFD 3D model using fitted intake pressure boundary conditions, compared to experimental results	102
4.6	Results for selected engine operating conditions	110
4.7	Summarize of the results	127
5	CONCLUSIONS	130
5.1	Future work proposals	131
	BIBLIOGRAPHY	132
A	DETAILED GEOMETRY	141
B	GRID DETAILED INFORMATION	144
B.1	Grid Refinement	144
B.2	Results for different grids	151
B.3	Time step	154
B.4	Conclusions of the grid dependence study	155

BIBLIOGRAPHY

- ALKIDAS, A. C. *Effects of Operational Parameters on Structural Temperatures and Coolant Heat Rejection of a SI Engine*. [S.l.], 1993.
- ALKIDAS, A. C. Combustion advancements in gasoline engines. *Energy Conversion and Management*, Elsevier, v. 48, n. 11, p. 2751–2761, 2007.
- ANGELBERGER, C.; POINSOT, T.; DELHAY, B. *Improving near-wall combustion and wall heat transfer modeling in SI engine computations*. [S.l.], 1997.
- BAI, C.; GOSMAN, A. Development of methodology for spray impingement simulation. *SAE transactions*, JSTOR, p. 550–568, 1995.
- BAKER, D.; ASSANIS, D. A methodology for coupled thermodynamic and heat transfer analysis of a diesel engine. *Applied Mathematical Modelling*, v. 18, p. 590–601, 1994.
- BARATTA, M.; RAPETTO, N. Fluid-dynamic and numerical aspects in the simulation of direct cng injection in spark-ignition engines. *Computers & Fluids*, Elsevier, v. 103, p. 215–233, 2014.
- BARROS, J. E. M. *Estudo de motores de combustão interna aplicando análise orientada a objetos*. Tese (Doutorado em Engenharia Mecânica) — Universidade Federal de Minas Gerais, Belo Horizonte, 2003.
- BAUMANN, M.; MARE, F. D.; JANICKA, J. On the validation of large eddy simulation applied to internal combustion engine flows part ii: numerical analysis. *Flow, turbulence and combustion*, Springer, v. 92, n. 1-2, p. 299–317, 2014.
- BAUMGARTEN, C. *Mixture Formation in Internal Combustion Engines*. Berlin Heidelberg: Springer-Verlag, 2006.
- BENAJES, J.; OLMEDA, P.; MARTÍN, J.; BLANCO-CAVERO, D.; WAREY, A. Evaluation of swirl effect on the global energy balance of a hmdi diesel engine. *Energy*, Elsevier, v. 122, p. 168–181, 2017.
- BERNARD, G.; LEBAS, R.; DEMOULIN, F.-X. A 0D phenomenological model using detailed tabulated chemistry methods to predict diesel combustion heat release and pollutant emissions. [S.l.], 2011.
- BERNI, F.; CICALESE, G.; FONTANESI, S. A modified thermal wall function for the estimation of gas-to-wall heat fluxes in cfd in-cylinder simulations of high performance spark-ignition engines. *Applied Thermal Engineering*, Elsevier, v. 115, p. 1045–1062, 2017.
- BOHAC, S. V.; BAKER, D. M.; ASSANIS, D. N. A global model for steady state and transient si engine heat transfer studies. *SAE transactions*, JSTOR, p. 196–214, 1996.
- BORMAN, G.; NISHIWAKI, K. Internal-combustion engine heat transfer. *Progress in Energy and Combustion Sciences*, v. 13, n. 1, p. 1–46, 1987.
- BROATCH, A.; OLMEDA, P.; MARGOT, X.; ESCALONA, J. New approach to study the heat transfer in internal combustion engines by 3d modelling. *International Journal of Thermal Sciences*, Elsevier, v. 138, p. 405–415, 2019.

- BROATCH P. OLMEDA, A. G. J. S. A.; WAREY, A. Impact of swirl on in-cylinder heat transfer in a light-duty diesel engine. *Energy*, v. 119, p. 1010–1023, 2017.
- BROEKAERT, S.; CUYPER, T. D.; PAEPE, M. D.; VERHELST, S. Experimental investigation of the effect of engine settings on the wall heat flux during hcci combustion. *Energy*, Elsevier, v. 116, p. 1077–1086, 2016.
- BROEKAERT, S.; DEMUYNCK, J.; CUYPER, T. D.; PAEPE, M. D.; VERHELST, S. Heat transfer in premixed spark ignition engines part i: Identification of the factors influencing heat transfer. *Energy*, Elsevier, v. 116, p. 380–391, 2016.
- BUHL, S.; DIETZSCH, F.; BUHL, C.; HASSE, C. Comparative study of turbulence models for scale-resolving simulations of internal combustion engine flows. *Computers & Fluids*, Elsevier, v. 156, p. 66–80, 2017.
- CD-ADAPCO. *STAR-CD Version 4.20*: Methodology for internal combustion engine applications. New York, 2013.
- CERDOUN, M.; CARCASCI, C.; GHENAIET, A. An approach for the thermal analysis of internal combustion engines' exhaust valves. *Applied Thermal Engineering*, Elsevier, v. 102, p. 1095–1108, 2016.
- CERIT, M.; COBAN, M. Temperature and thermal stress analyses of a ceramic-coated aluminum alloy piston used in a diesel engine. *International Journal of Thermal Sciences*, Elsevier, v. 77, p. 11–18, 2014.
- CEVIZ, M. Intake plenum volume and its influence on the engine performance, cyclic variability and emissions. *Energy Conversion and Management*, Elsevier, v. 48, n. 3, p. 961–966, 2007.
- CLENCI, A. C.; IORGA-SIMĂN, V.; DELIGANT, M.; PODEVIN, P.; DESCOMBES, G.; NICULESCU, R. A cfd (computational fluid dynamics) study on the effects of operating an engine with low intake valve lift at idle corresponding speed. *Energy*, Elsevier, v. 71, p. 202–217, 2014.
- COLIN, O.; BENKENIDA, A. The 3-zones extended coherent flame model (ecfm-3z) for computing premixed/diffusion combustion. *Oil & Gas Science and Technology*, EDP Sciences, v. 59, n. 6, p. 593–609, 2004.
- COLIN, O.; BENKENIDA, A.; ANGELBERGER, C. 3d modeling of mixing, ignition and combustion phenomena in highly stratified gasoline engines. *Oil & gas science and technology*, EDP Sciences, v. 58, n. 1, p. 47–62, 2003.
- COSTA, R. B. R. da. *Estudo experimental da tecnologia dual-fuel em motor de combustão interna utilizando biogás, GNV e etanol*. Dissertação (Mestrado em Engenharia Mecânica) — Universidade Federal de Minas Gerais, Belo Horizonte, 2017.
- CUYPER, T. D.; BROEKAERT, S.; CHANA, K.; PAEPE, M. D.; VERHELST, S. Evaluation of empirical heat transfer models using tfg heat flux sensors. *Applied Thermal Engineering*, Elsevier, v. 118, p. 561–569, 2017.
- DENG, B.; FU, J.; ZHANG, D.; YANG, J.; FENG, R.; LIU, J.; LI, K.; LIU, X. The heat release analysis of bio-butanol/gasoline blends on a high speed si (spark ignition) engine. *Energy*, Elsevier, v. 60, p. 230–241, 2013.

- DENG, X.; LEI, J.; WEN, J.; WEN, Z.; SHEN, L. Numerical investigation on the oscillating flow and uneven heat transfer processes of the cooling oil inside a piston gallery. *Applied Thermal Engineering*, Elsevier, v. 126, p. 139–150, 2017.
- DRAKE, M.; HAWORTH, D. Advanced gasoline engine development using optical diagnostics and numerical modeling. *Proceedings of the Combustion Institute*, Elsevier, v. 31, n. 1, p. 99–124, 2007.
- DUCLOS, J.; ZOLVER, M.; BARITAUD, T. 3d modeling of combustion for di-si engines. *Oil & Gas Science and Technology*, EDP Sciences, v. 54, n. 2, p. 259–264, 1999.
- DUDAREVA, N. Y.; ENIKEEV, R.; IVANOV, V. Y. Thermal protection of internal combustion engines pistons. *Procedia Engineering*, Elsevier, v. 206, p. 1382–1387, 2017.
- EÇA, L.; HOEKSTRA, M. A procedure for the estimation of the numerical uncertainty of cfd calculations based on grid refinement studies. *Journal of Computational Physics*, Elsevier, v. 262, p. 104–130, 2014.
- FAN, X.; CHE, Z.; WANG, T.; LU, Z. Numerical investigation of boundary layer flow and wall heat transfer in a gasoline direct-injection engine. *International Journal of Heat and Mass Transfer*, Elsevier, v. 120, p. 1189–1199, 2018.
- FINLAY, I.; GALLACHER, G.; BIDDULPH, T.; MARSHALL, R. The application of precision cooling to the cylinder-head of a small, automotive, petrol engine. *SAE transactions*, JSTOR, p. 399–410, 1988.
- FINOL, C.; ROBINSON, K. Thermal modelling of modern engines: a review of empirical correlations to estimate the in-cylinder heat transfer coefficient. *Proceedings of the institution of mechanical engineers, part D: journal of automobile engineering*, Sage Publications Sage UK: London, England, v. 220, n. 12, p. 1765–1781, 2006.
- FONSECA, L.; OLMEDA, P.; NOVELLA, R.; VALLE, R. M. Internal combustion engine heat transfer and wall temperature modeling: An overview. *Archives of Computational Methods in Engineering*, Oct 2019. ISSN 1886-1784.
- FONSECA, L. G. *Caracterização do escoamento de ar em um motor de combustão interna utilizando mecânica dos fluidos computacional*. Dissertação (Mestrado em Engenharia Mecânica) — Universidade Federal de Minas Gerais, Belo Horizonte, 2014.
- GE, H.-W.; SHI, Y.; REITZ, R. D.; WICKMAN, D. D.; WILLEMS, W. Optimization of a hmdi diesel engine for passenger cars using a multi-objective genetic algorithm and multi-dimensional modeling. *SAE International Journal of Engines*, JSTOR, v. 2, n. 1, p. 691–713, 2009.
- GIANNAKOPOULOS, G.; FROUZAKIS, C. E.; BOULOUCHOS, K.; FISCHER, P. F.; TOMBOULIDES, A. Direct numerical simulation of the flow in the intake pipe of an internal combustion engine. *International Journal of Heat and Fluid Flow*, Elsevier, v. 68, p. 257–268, 2017.
- GÜRBÜZ, H. Parametrical investigation of heat transfer with fast response thermocouple in si engine. *Journal of Energy Engineering*, v. 142, n. 4, p. 04016014, 2016.

- HAN, Z.; PARRISH, S. E.; FARRELL, P. V.; REITZ, R. D. Modeling atomization processes of pressure-swirl hollow-cone fuel sprays. *Atomization and sprays*, Begel House Inc., v. 7, n. 6, 1997.
- HAN, Z.; REITZ, R. D. Turbulence modeling of internal combustion engines using RNG κ - ϵ models. *Combustion science and technology*, Taylor & Francis, v. 106, n. 4-6, p. 267–295, 1995.
- HAN, Z.; REITZ, R. D. A temperature wall function formulation for variable-density turbulent flows with application to engine convective heat transfer modeling. *International journal of heat and mass transfer*, Elsevier, v. 40, n. 3, p. 613–625, 1997.
- HANRIOT, S. d. M.; QUEIROZ, J. M.; MAIA, C. B. Effects of variable-volume helmholtz resonator on air mass flow rate of intake manifold. *Journal of the Brazilian Society of Mechanical Sciences and Engineering*, Springer, v. 41, n. 2, p. 79, 2019.
- HANRIOT, S. de M. *Estudo dos fenômenos pulsantes do escoamento de ar nos condutos de admissão em motores de combustão interna*. Tese (Doutorado em Engenharia Mecânica) — Universidade Federal de Minas Gerais, Belo Horizonte, 2001.
- HASSE, C. Scale-resolving simulations in engine combustion process design based on a systematic approach for model development. *International Journal of Engine Research*, SAGE Publications Sage UK: London, England, v. 17, n. 1, p. 44–62, 2016.
- HEYWOOD, J. B. Engine combustion modelling - an overview. In: SPRINGER US. *Combustion modeling in reciprocating engines*. New York, 1980.
- HEYWOOD, J. B. *Internal Combustion Engine Fundamentals*. New York: McGraw-Hill, 2018.
- INAGAKI, M.; NAGAOKA, M.; HORINOUCHI, N.; SUGA, K. Large eddy simulation analysis of engine steady intake flows using a mixed-time-scale subgrid-scale model. *International Journal of Engine Research*, SAGE Publications Sage UK: London, England, v. 11, n. 3, p. 229–241, 2010.
- INCROPERA, F. P.; LAVINE, A. S.; BERGMAN, T. L.; DEWITT, D. P. *Fundamentals of heat and mass transfer*. [S.I.]: Wiley, 2007.
- IRIMESCU, A.; MEROLA, S. S.; TORNATORE, C.; VALENTINO, G. Development of a semi-empirical convective heat transfer correlation based on thermodynamic and optical measurements in a spark ignition engine. *Applied Energy*, Elsevier, v. 157, p. 777–788, 2015.
- JAMES, E. H. *Combustion modelling in spark ignition engines*. 1984.
- JEEVANASHANKARA; MADHUSUDANA, C.; KULKARNI, M. Thermal contact conductances of metallic contacts at low loads. *Applied Energy*, v. 35, n. 2, p. 151 – 164, 1990.
- JEMNI, M. A.; KANTCHEV, G.; ABID, M. S. Influence of intake manifold design on in-cylinder flow and engine performances in a bus diesel engine converted to lpg gas fuelled, using cfd analyses and experimental investigations. *Energy*, Elsevier, v. 36, n. 5, p. 2701–2715, 2011.
- JOINT COMMITTEE FOR GUIDES IN METROLOGY. *JCGM 100:2008: Evaluation of measurement data - guide to the expression of uncertainty in measurement*. [S.I.], 2008. 120 p.

- KHALILARYA, S.; NEMATI, A. et al. A numerical investigation on the influence of egr in a supercharged si engine fueled with gasoline and alternative fuels. *Energy conversion and management*, Elsevier, v. 83, p. 260–269, 2014.
- KIKUSATO, A.; KUSAKA, J.; DAISHO, Y. *A Numerical Study on Predicting Combustion Chamber Wall Surface Temperature Distributions in a Diesel Engine and their Effects on Combustion, Emission and Heat Loss Characteristics by Using a 3D-CFD Code Combined with a Detailed Heat Transfer Model*. [S.l.], 2015.
- LI, Y.; KONG, S.-C. Coupling conjugate heat transfer with in-cylinder combustion modeling for engine simulation. *International Journal of Heat and Mass Transfer*, Elsevier, v. 54, n. 11-12, p. 2467–2478, 2011.
- LINSE, D.; KLEEMANN, A.; HASSE, C. Probability density function approach coupled with detailed chemical kinetics for the prediction of knock in turbocharged direct injection spark ignition engines. *Combustion and Flame*, Elsevier, v. 161, n. 4, p. 997–1014, 2014.
- LIU, Y.; GUESSOUS, L.; SANGEORZAN, B.; ALKIDAS, A. Laboratory experiments on oil-jet cooling of internal combustion engine pistons: Area-average correlation of oil-jet impingement heat transfer. *Journal of Energy Engineering*, American Society of Civil Engineers, v. 141, n. 2, p. C4014003, 2014.
- LU, Y.; ZHANG, X.; XIANG, P.; DONG, D. Analysis of thermal temperature fields and thermal stress under steady temperature field of diesel engine piston. *Applied Thermal Engineering*, Elsevier, v. 113, p. 796–812, 2017.
- LV, J.; WANG, P.; BAI, M.; LI, G.; ZENG, K. Experimental visualization of gas–liquid two-phase flow during reciprocating motion. *Applied Thermal Engineering*, Elsevier, v. 79, p. 63–73, 2015.
- MA, P. C.; EWAN, T.; JAINSKI, C.; LU, L.; DREIZLER, A.; SICK, V.; IHME, M. Development and analysis of wall models for internal combustion engine simulations using high-speed micro-piv measurements. *Flow, Turbulence and Combustion*, Springer, v. 98, n. 1, p. 283–309, 2017.
- MANDANIS, C.; SCHMITT, M.; KOCH, J.; WRIGHT, Y. M.; BOULOUCHOS, K. Wall heat flux and thermal stratification investigations during the compression stroke of an engine-like geometry: A comparison between les and dns. *Flow, Turbulence and Combustion*, Springer, v. 100, n. 3, p. 769–795, 2018.
- MARE, F. di; KNAPPSTEIN, R. Statistical analysis of the flow characteristics and cyclic variability using proper orthogonal decomposition of highly resolved les in internal combustion engines. *Computers & Fluids*, Elsevier, v. 105, p. 101–112, 2014.
- MARE, F. di; KNAPPSTEIN, R.; BAUMANN, M. Application of les-quality criteria to internal combustion engine flows. *Computers & Fluids*, Elsevier, v. 89, p. 200–213, 2014.
- MASOULEH, M. G.; KESKINEN, K.; KAARIO, O.; KAHILA, H.; WRIGHT, Y. M.; VUORINEN, V. Flow and thermal field effects on cycle-to-cycle variation of combustion: scale-resolving simulation in a spark ignited simplified engine configuration. *Applied energy*, Elsevier, v. 230, p. 486–505, 2018.

- MEHDIPOUR, R.; BANIAMERIAN, Z.; DELAURÉ, Y. Three dimensional simulation of nucleate boiling heat and mass transfer in cooling passages of internal combustion engines. *Heat and Mass Transfer*, Springer, v. 52, n. 5, p. 957–968, 2016.
- MELO, T. C. C. de. *Análise experimental e simulação computacional de um motor flex operando com diferentes misturas de etanol hidratado na gasolina*. Tese (Doutorado em Engenharia Mecânica) — Universidade Federal do Rio de Janeiro, Rio de Janeiro, 2012.
- MENEVEAU, C.; POINSOT, T. Stretching and quenching of flamelets in premixed turbulent combustion. *Combustion and Flame*, Elsevier, v. 86, n. 4, p. 311–332, 1991.
- MEZHER, H.; CHALET, D.; MIGAUD, J.; CHESSE, P. Frequency based approach for simulating pressure waves at the inlet of internal combustion engines using a parameterized model. *Applied energy*, Elsevier, v. 106, p. 275–286, 2013.
- MICHL, J.; NEUMANN, J.; ROTTENGRUBER, H.; WENSING, M. Derivation and validation of a heat transfer model in a hydrogen combustion engine. *Applied Thermal Engineering*, Elsevier, v. 98, p. 502–512, 2016.
- MILLO, F.; LUISI, S.; BOREAN, F.; STROPIANA, A. Numerical and experimental investigation on combustion characteristics of a spark ignition engine with an early intake valve closing load control. *Fuel*, Elsevier, v. 121, p. 298–310, 2014.
- MISDARIIS, A.; VERMOREL, O.; POINSOT, T. Les of knocking in engines using dual heat transfer and two-step reduced schemes. *Combustion and Flame*, Elsevier, v. 162, n. 11, p. 4304–4312, 2015.
- NETTO, N. A. D. *Estudo experimental de tecnologias que visam a maximização da eficiência de conversão de combustível em um motor monocilindro de pesquisa*. Dissertação (Mestrado em Engenharia Mecânica) — Universidade Federal de Minas Gerais, Belo Horizonte, 2018.
- NIJEWEME, D. O.; KOK, J.; STONE, C.; WYSZYNSKI, L. Unsteady in-cylinder heat transfer in a spark ignition engine: experiments and modelling. *Proceedings of the Institution of Mechanical Engineers, Part D: Journal of Automobile Engineering*, Sage Publications Sage UK: London, England, v. 215, n. 6, p. 747–760, 2001.
- OLMEDA, P.; MARTÍN, J.; NOVELLA, R.; CARREÑO, R. An adapted heat transfer model for engines with tumble motion. *Applied energy*, Elsevier, v. 158, p. 190–202, 2015.
- PARIOTIS E.G., K. G.; RAKOPOULOS, C. Comparative analysis of three simulation models applied on a motored internal combustion engine. *Energy Conversion and Management*, v. 60, p. 45–55, 2012.
- PEREIRA, L. V. M. *Estudo Experimental da Influência de um Ressonador de Volume Variável na Massa de Ar Admitida por um Motor de Combustão Interna*. Tese (Doutorado em Engenharia Mecânica) — Universidade Federal de Minas Gerais, Belo Horizonte, 2008.
- PERINI, F.; MILES, P. C.; REITZ, R. D. A comprehensive modeling study of in-cylinder fluid flows in a high-swirl, light-duty optical diesel engine. *Computers & Fluids*, Elsevier, v. 105, p. 113–124, 2014.
- PIEDRAHITA, C. A. R. *Contribución al conocimiento del comportamiento térmico y la gestión térmica de los motores de combustión interna alternativos*. Tese (Doutorado) — Universitat Politècnica de València, 2009.

- QI, Y.; DONG, L.; LIU, H.; PUZINAUSKAS, P.; MIDKIFF, K. Optimization of intake port design for si engine. *International Journal of Automotive Technology*, Springer, v. 13, n. 6, p. 861–872, 2012.
- RAMOS, J. I. *Internal combustion engine modelling*. New York: CRC Press, 1989.
- RANZ, W.; MARSHALL, W. R. et al. Evaporation from drops. *Chem. eng. prog.*, v. 48, n. 3, p. 141–146, 1952.
- RASHEDUL, H.; KALAM, M.; MASJUKI, H.; ASHRAFUL, A.; IMTENAN, S.; SAJJAD, H.; WEE, L. Numerical study on convective heat transfer of a spark ignition engine fueled with bioethanol. *International Communications in Heat and Mass Transfer*, Elsevier, v. 58, p. 33–39, 2014.
- REITZ, R. et al. Modeling atomization processes in high-pressure vaporizing sprays. *Atomisation and Spray Technology*, v. 3, n. 4, p. 309–337, 1987.
- ROBERT, A.; RICHARD, S.; COLIN, O.; MARTINEZ, L.; FRANCQUEVILLE, L. D. Les prediction and analysis of knocking combustion in a spark ignition engine. *Proceedings of the Combustion Institute*, Elsevier, v. 35, n. 3, p. 2941–2948, 2015.
- ROSA, N.; VILLEDIEU, P.; DEWITTE, J.; LAVERGNE, G. A new droplet-wall interaction model. *ICLASS06-167*, ICLASS-2006, 2006.
- SAKOWITZ, A.; MIHAESCU, M.; FUCHS, L. Flow decomposition methods applied to the flow in an ic engine manifold. *Applied Thermal Engineering*, Elsevier, v. 65, n. 1-2, p. 57–65, 2014.
- ŠARIĆ, S.; BASARA, B.; ŽUNIĆ, Z. Advanced near-wall modeling for engine heat transfer. *International Journal of Heat and Fluid Flow*, Elsevier, v. 63, p. 205–211, 2017.
- SCHIFFMANN, P.; GUPTA, S.; REUSS, D.; SICK, V.; YANG, X.; KUO, T.-W. Tcc-iii engine benchmark for large-eddy simulation of ic engine flows. *Oil & Gas Science and Technology*, EDP Sciences, v. 71, n. 1, 2016.
- SCHMITT, M.; BOLOUCHOS, K. Role of the intake generated thermal stratification on the temperature distribution at top dead center of the compression stroke. *International Journal of Engine Research*, SAGE Publications Sage UK: London, England, v. 17, n. 8, p. 836–845, 2016.
- SCHMITT, M.; FROUZAKIS, C. E.; TOMBOULIDES, A. G.; WRIGHT, Y. M.; BOLOUCHOS, K. Direct numerical simulation of the effect of compression on the flow, temperature and composition under engine-like conditions. *Proceedings of the Combustion Institute*, Elsevier, v. 35, n. 3, p. 3069–3077, 2015.
- SCHMITT, M.; FROUZAKIS, C. E.; WRIGHT, Y. M.; TOMBOULIDES, A. G.; BOLOUCHOS, K. Direct numerical simulation of the compression stroke under engine-relevant conditions: Evolution of the velocity and thermal boundary layers. *International Journal of Heat and Mass Transfer*, Elsevier, v. 91, p. 948–960, 2015.
- SCHMITT, M.; FROUZAKIS, C. E.; WRIGHT, Y. M.; TOMBOULIDES, A.; BOLOUCHOS, K. Direct numerical simulation of the compression stroke under engine relevant conditions: Local wall heat flux distribution. *International Journal of Heat and Mass Transfer*, Elsevier, v. 92, p. 718–731, 2016.

- SCHMITT, M.; FROUZAKIS, C. E.; WRIGHT, Y. M.; TOMBOULIDES, A. G.; BOLOUCHOS, K. Investigation of wall heat transfer and thermal stratification under engine-relevant conditions using dns. *International Journal of Engine Research*, SAGE Publications Sage UK: London, England, v. 17, n. 1, p. 63–75, 2016.
- SILVA, E.; OCHOA, A.; HENRÍQUEZ, J. Analysis and runners length optimization of the intake manifold of a 4-cylinder spark ignition engine. *Energy Conversion and Management*, Elsevier, v. 188, p. 310–320, 2019.
- SOUZA, G. R. de; PELLEGRINI, C. de C.; FERREIRA, S. L.; PAU, F. S.; ARMAS, O. Study of intake manifolds of an internal combustion engine: A new geometry based on experimental results and numerical simulations. *Thermal Science and Engineering Progress*, Elsevier, v. 9, p. 248–258, 2019.
- TANOV, S.; SALVADOR-IBORRA, J.; ANDERSSON, Ö.; OLMEDA, P.; GARCÍA, A. Influence of the number of injections on piston heat rejection under low temperature combustion conditions in an optical compression-ignition engine. *Energy Conversion and Management*, Elsevier, v. 153, p. 335–345, 2017.
- TAYLOR, G. I. The instability of liquid surfaces when accelerated in a direction perpendicular to their planes. i. *Proceedings of the Royal Society of London. Series A. Mathematical and Physical Sciences*, The Royal Society London, v. 201, n. 1065, p. 192–196, 1950.
- THE AMERICAN SOCIETY OF MECHANICAL ENGINEERS. ASME V&V 20-2009: Standard for verification and validation in computational fluid dynamics and heat transfer. New York, 2009. 88 p.
- TOOSI, A. N.; FAROKHI, M.; MASHADI, B. Application of modified eddy dissipation concept with large eddy simulation for numerical investigation of internal combustion engines. *Computers & Fluids*, Elsevier, v. 109, p. 85–99, 2015.
- TORREGROSA, A.; BROATCH, A.; OLMEDA, P.; CORNEJO, O. Experiments on subcooled flow boiling in ic engine-like conditions at low flow velocities. *Experimental Thermal and Fluid Science*, Elsevier, v. 52, p. 347–354, 2014.
- TORREGROSA, A.; BROATCH, A.; OLMEDA, P.; SALVADOR-IBORRA, J.; WAREY, A. Experimental study of the influence of exhaust gas recirculation on heat transfer in the firedeck of a direct injection diesel engine. *Energy Conversion and Management*, Elsevier, v. 153, p. 304–312, 2017.
- TORREGROSA, A.; OLMEDA, P.; DEGRAEUWE, B.; REYES, M. A concise wall temperature model for di diesel engines. *Applied Thermal Engineering*, Elsevier, v. 26, n. 11-12, p. 1320–1327, 2006.
- TORREGROSA, P.; OLMEDA, J. M. A.; ROMERO, C. A tool for predicting the thermal performance of a diesel engine. *Heat Transfer Engineering*, v. 32, n. 10, p. 891–904, 2011.
- VERSTEEG, H. K.; MALALASEKERA, W. *An introduction to computational fluid dynamics: the finite volume method*. [S.l.]: Pearson education, 2007.
- WAKIL, M. M. E.; UYEHARA, O.; MYERS, P. *A theoretical investigation of the heating-up period of injected fuel droplets vaporizing in air*. [S.l.], 1954.

- WANG, P.; HAN, K.; YOON, S.; YU, Y.; LIU, M. The gas-liquid two-phase flow in reciprocating enclosure with piston cooling gallery application. *International Journal of Thermal Sciences*, Elsevier, v. 129, p. 73–82, 2018.
- WANG, P.; LIANG, R.; YU, Y.; ZHANG, J.; LV, J.; BAI, M. The flow and heat transfer characteristics of engine oil inside the piston cooling gallery. *Applied Thermal Engineering*, Elsevier, v. 115, p. 620–629, 2017.
- WANG, T.; LI, W.; JIA, M.; LIU, D.; QIN, W.; ZHANG, X. Large-eddy simulation of in-cylinder flow in a disi engine with charge motion control valve: Proper orthogonal decomposition analysis and cyclic variation. *Applied Thermal Engineering*, Elsevier, v. 75, p. 561–574, 2015.
- WOSCHNI, G. A universally applicable equation for the instantaneous heat transfer coefficient in the internal combustion engine. [S.l.], 1967.
- XING, T. A general framework for verification and validation of large eddy simulations. *Journal of Hydrodynamics*, Springer, v. 27, n. 2, p. 163–175, 2015.
- YAKHOT, V.; ORSZAG, S.; THANGAM, S.; GATSKI, T.; SPEZIALE, C. Development of turbulence models for shear flows by a double expansion technique. *Physics of Fluids A: Fluid Dynamics*, AIP, v. 4, n. 7, p. 1510–1520, 1992.
- YAKHOT, V.; ORSZAG, S. A. Renormalization group analysis of turbulence. i. basic theory. *Journal of scientific computing*, Springer, v. 1, n. 1, p. 3–51, 1986.
- YAMAKAWA, M.; YOUSO, T.; FUJIKAWA, T.; NISHIMOTO, T.; WADA, Y. ; SATO, K.; YOKOHATA, H. Combustion technology development for a high compression ratio si engine. *SAE International Journal of Fuels and Lubricants*, JSTOR, v. 5, n. 1, p. 98–105, 2012.
- ZHANG, L. Parallel simulation of engine in-cylinder processes with conjugate heat transfer modeling. *Applied Thermal Engineering*, Elsevier, v. 142, p. 232–240, 2018.